Selectivity of Auger Decays to the Local Surface Environment

M. I. Trioni,[1] S. Caravati,[1,2] G. P. Brivio,[1,2] L. Floreano,[3] F. Bruno,[3] and A. Morgante[3,4]

[1]*Istituto Nazionale per la Fisica della Materia, UdR Milano Bicocca, via Cozzi 53, I-20125 Milano, Italy*
[2]*Dipartimento di Scienza dei Materiali, Università di Milano-Bicocca, via Cozzi 53, I-20125 Milano, Italy*
[3]*Laboratorio TASC, Istituto Nazionale per la Fisica della Materia, Basovizza SS14 Km 163.5, I-34012 Trieste, Italy*
[4]*Dipartimento di Fisica, Università di Trieste, via Valerio 2, I-34100 Trieste, Italy*

(Received 8 March 2004; published 11 November 2004)

The line shape of the Auger decay of adatoms is studied by a joint theoretical and experimental effort, the former within a DFT framework, and the latter with synchrotron radiation measurements. We investigate the $KL_{2,3}V$ Auger deexcitation of Na on Al(111), a system with different adsorption geometries. In particular, we study the $(\sqrt{3} \times \sqrt{3})R30^\circ$ phase at 1/3 ML (monolayer) and the more complex (2×2) structure at 1/2 ML coverage. From the comparison between theory and experiment, we unambiguously determine features that allow for the determination of the adsorption environment from the adatom Auger spectrum.

DOI: 10.1103/PhysRevLett.93.206802 PACS numbers: 73.20.Hb, 32.80.Hd, 71.15.Mb, 82.80.Pv

Relaxation of excited many-electron systems often proceeds via nonradiative transitions. A fundamental phenomenon is the Auger decay, which originates once a core atomic level is ionized by an external probe. It involves the transitions of two less tightly bound electrons, one filling the inner hole and the other one escaping into vacuum. Several research efforts on the Auger effect are being performed in a variety of fields. For example, a deeper understanding of the Auger dynamics currently motivates frontier time-resolved experiments in core-excited atoms [1] and in quantum dots for Auger-like electron-hole recombinations [2]. In a solid, the emitted electrons give a very surface sensitive signal due to their short escape depth of the order of 1–2 nm. For this reason, Auger electron energies are widely used to study the chemical composition of surfaces and their shifts with respect to bulk spectra convey relevant information on bonding [3]. If the valence electrons participate in the Auger process as in core-core-valence (CCV) transitions, the shape of the Auger peaks transforms into broader bands. Such features account for the local density of states (LDOS) around a core ionized atom, and for correlation properties like plasmon satellites. However, if one could make up a method capable also to derive structural properties from the Auger decay line shapes, i.e., to determine different surface reconstruction and adsorption geometries, this result would significantly extend the applicability of Auger spectroscopy to the surface microscopic analysis.

In this Letter we address the above issue by a joint theoretical and experimental investigation. We study Na/Al(111), a system in which different Na adsorption geometries, on changing the adatom fractional coverage and the substrate growth temperature, are known from previous experiments and calculations [4–7]. We concentrate on the CCV Auger line shapes of electronically excited Na atoms. In fact, CCV spectra of alkali metals can be taken into account accurately in the Kohn-Sham scheme of the density functional theory (DFT), since hole-hole correlation effects in the final state are negligible, and the system may be assumed to be in a relaxed quasi ground state with a core hole on the adatom [8]. In such a framework, we have calculated the Auger profiles of Na adsorbed at different sites via the excited state LDOS [9,10]. From the experimental point of view we have exploited last generation synchrotron radiation facilities, which allow for obtaining the very weak CCV signal of the adatoms. In this way such Auger profiles and their dependence on the Na adsorption geometry have been measured in an unambiguous way. We have found that the experimental Auger spectra are in excellent agreement with the theoretical ones.

To calculate the CCV Auger rates, one could apply the Fermi golden rule. But such a method is often a cumbersome and a computationally demanding one, especially when the structure of the surface unit cell is to be taken into account in a realistic manner. We determined instead the transition rates of an adsorbate by using the simpler approximate expression given by [11]

$$P(E) = \sum_l M_l D_l(E_v), \tag{1}$$

where the energy E of the Auger electron is equal to $E = E_{c_f} - E_{c_i} + E_v$. E_{c_i} and E_{c_f} are the energies of the initial and final core hole, respectively, while E_v is that of the valence electron, all of them referred to the Fermi level. The factors M_l are energy independent terms involving a valence electronic state of orbital character l, and $D_l(E_v)$ is the corresponding orbital resolved valence LDOS in a localized volume around the ionized impurity. We proceed as follows: first we perform a DFT calculation of the adatom, with a core hole, on a jellium surface and fit the impurity Auger rates worked out by Eq. (1) to those obtained exactly by the Fermi golden rule. The relevant physical parameter of the approximate approach is the radius R_{cut} of a sphere centered on the adatom, inside

which we compute the excited LDOS. The factors M_l follow as by-product. We have numerically proven that the Auger rates from Eq. (1) fit the exact ones for a jellium host [10]. We observe that R_{cut} depends on the spatial extent of the Auger coupling terms, which is essentially determined by the range of the adatom core wave functions; consequently, such cutoff radius is a property of the chemical species, regardless of the substrate and the impurity site (bulk, subsurface, or onsurface). Second, we compute the LDOS of the excited adatom within a sphere with radius R_{cut}, but on a realistic substrate. The DFT calculations are performed in the local density approximation by using the Green function embedding method [12,13]. Finally, we obtain the Auger profiles by convolving the rates in Eq. (1) with a Lorentzian, accounting for hole lifetime, and a Gaussian, for instrumental broadening.

The experiments have been carried out at the INFM-ALOISA beam line installed at the Elettra Synchrotron in Trieste, whose monochromator yields a large photon flux in the 1500 eV range, most useful for the present experiment [14]. The Auger spectra have been taken by orienting the sample in transverse magnetic p polarization and at a fixed grazing angle of $\sim 1.5\,^{\circ}$, while keeping one electron spectrometer along the surface normal direction. The Al(111) sample was prepared by repeated cycles of 800 eV Ar^{+} sputtering and annealing to 670 K. Surface cleanness and order where checked by x-ray photoelectron spectroscopy (XPS) and reflection high-energy electron diffraction (RHEED). The Na cell evaporation rate was calibrated by both XPS and RHEED in agreement with previous findings [4]. The Na $2p$ photoemission spectra for a few representative depositions and temperatures are shown in Fig. 1. The calculated (see below for details) XPS energies, which are denoted by arrows, are very close to the experimental ones. At Na coverage of $1/3$ ML (monolayer), only one $2p$ component is observed in XPS, but with a core level shift toward lower binding energy for the low temperature (LT) film at 150 K. The room temperature (RT) film shows instead an additional $2p$ component at 490 meV lower binding energy, when further Na is evaporated up to the saturation coverage. Several investigations argue that LT deposition produces Na adsorption on top of Al(111) [4]. Deposition at RT creates first a $(\sqrt{3} \times \sqrt{3})R30\,^{\circ}$ phase at $1/3$ ML, then a (2×2) phase at the saturation coverage of $1/2$ ML. As opposed to LT deposition, Na and Al intermixing always occurs for RT deposition. In particular, the $1/3$ ML RT phase is formed by the substitution of one Al atom by Na every three surface unit cells [5]. For the (2×2) phase, two distinct Na adsorption sites are observed by the core level shift of the Na $2p$ photoemission spectrum [4]. Most authors agree on a two-layer Na-Al surface alloy, where the bottom layer Na atoms are substitutional [6,15,16] and the upper Na-Al layer is formed by Na

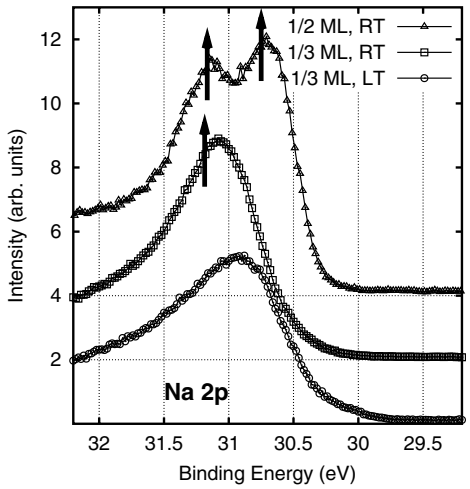

FIG. 1. Na $2p$ photoemission spectra taken with a photon energy of 150 eV and overall energy resolution better than 325 meV for the upper spectrum and 450 meV for the other two. RT spectra at $1/2$ ML (saturation coverage) [(2×2) phase], RT spectra at $1/3$ ML [$(\sqrt{3} \times \sqrt{3})R30\,^{\circ}$ phase], and LT spectra at $1/3$ ML are shown from top to bottom. The arrows identify the DFT energies.

atoms in fcc sites and Al atoms in hcp ones, as indicated by LEED and surface extended x-ray absorption fine structure (SEXAFS) studies [6], also supported by *ab-initio* calculations [7].

The measurement of the Na KLV Auger spectra is a difficult task due to three concurrent factors: (i) the decay rate is very small as compared with KLL transitions that dominate the Auger spectrum; (ii) the Na signal arises from a tiny amount of atoms, since we are considering structures in the submonolayer range; and (iii) the background is strongly affected by the Al L-shell photoemission, whose plasmons are also very intense and numerous. In the experiments, the incidence angle was kept at the critical value ($\sim 1.5\,^{\circ}$) to enhance the signal from Na. We selected a photon energy of 1340 eV. As the Auger line shape is unaffected by the photon energy resolution (~ 8 eV), the acquisition statistics of the KLV peaks was improved by decreasing the photon bandwidth to $\sim 0.6\%$, corresponding to a photon flux of $\sim 5 \times 10^{11}$ ph/sec. On the other hand, we have kept the electron energy resolution to about 0.65 eV, which is acceptable to measure the Auger line shape. The acquisition time for each Na KLV spectrum was ~ 14 min. Finally, about 50 spectra have been taken for each Na phase. The measured KLV spectra are displayed in Fig. 2, before background subtraction. The latter was obtained by measuring the spectrum on the clean substrate in the same experimental condition. The $1/3$ ML films at LT and RT are very similar, reflecting the low degree of penetration of the Na atoms in the substrate lattice in both cases. To demonstrate that the Auger peaks strongly depend on the adsorption geometry, it is most interesting to restrict

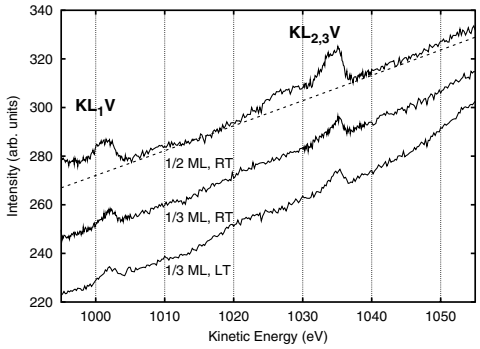

FIG. 2. The Na KLV Auger spectra taken from three different Na films. From top to bottom: the (2×2) phase for $1/2$ ML of Na deposited at RT; the $(\sqrt{3} \times \sqrt{3})R30\,^\circ$ phase for $1/3$ ML of Na at RT; the phase for $1/3$ ML of Na at LT. The spectra have been taken keeping the sample at the same temperature of the corresponding deposition. The dashed line is the background from the clean Al(111) surface.

our analysis to the two RT phases, which present different Na sites in the reconstructed surface layers of Al(111) [4]. We shall concentrate on the $KL_{2,3}V$ peak, since experimental data of the more intense KLL transition partially overlap on those of the KL_1V one, hence the analysis may result less transparent. In this respect, the most striking result of this Letter is displayed in Fig. 2, namely, the clear difference between the Auger spectra of the films of Na at $1/3$ ML and at saturation, the latter exhibiting a shoulder on the $KL_{2,3}V$ peak at $\sim$1.5 eV lower energy (see also Fig. 4). The weak bump at $\sim$1027 eV in the $1/2$ ML spectrum at RT is due to a small amount of sodium oxide, whose formation has been observed to be faster than for the $1/3$ ML surface. However, thanks to the large energy shift (~ -8 eV) of the oxide, the Auger line originated by Na atoms in the (2×2) phase is mostly unaffected, its low energy tail only being slightly distorted.

We have evaluated the electronic properties by assuming the structural models of Refs. [5–7] for the two RT phases. The computation is based on a full-potential linearized augmented plane wave (FLAPW) scheme of embedding, as implemented in the code described in Ref. [13]. The ground state and the excited state LDOS's with a $1s$ core hole on the adatom are worked out by solving the Kohn-Sham equation in an embedding region containing the uppermost reconstructed and relaxed layers of both phases ($\sim$10 Bohr thick) plus vacuum. We have verified that one obtains the same excited LDOS's with a hole in the final $2p$ state. In the calculation of the Auger rates by Eq. (1), the cutoff radius of the LDOS volume is $R_{\mathrm{cut}} = 2.14$ Bohr around Na and the ratio $M_s/M_p = 0.455$ (note that only s and p components are needed for Na) [10]. The energy difference $E_{c_f} - E_{c_i}$ entering Eq. (1) has been determined from that of the Kohn-Sham eigenvalues ($\epsilon_{2p} - \epsilon_{1s}$) by applying the transition state theory to both the $1s$ and the $2p$ levels of Na in a self-consistent spin polarized calculation within our DFT approach [17]. Note that also the $2p$ XPS DFT peaks of Na in Fig. 1 have been obtained by transition state theory.

In Fig. 3 we report the calculated LDOS's. For the $(\sqrt{3} \times \sqrt{3})R30\,^\circ$ reconstruction, the ground state and the excited state LDOS's are displayed in the panels (a) and (b), respectively. For the (2×2) phase, panel (c) shows the LDOS for the excited inner Na atom, while panel (d) that for the outer Na one. Comparison between the LDOS's in the upper panels show that the presence of a core hole on Na increases the number of states below the Fermi level, in particular, of the s component, whose peak is shifted down in agreement with previous calculations [9,18]. We have verified the same behavior by comparing the ground state and the excited LDOS's of the Na (2×2) phase. Whereas both panels (b) and (d) are fairly similar because of the almost equivalent environment of the Na impurities, the LDOS of panel (c) is differently shaped, with a peak at lower energy. This is due to a much stronger hybridization between the s state of Na and the Al substrate being Na a subsurface impurity. The differences among the LDOS's in panels (b), (c), and (d) suggest that Auger spectra, calculated by using such l-decomposed LDOS's via Eq. (1), should be different and

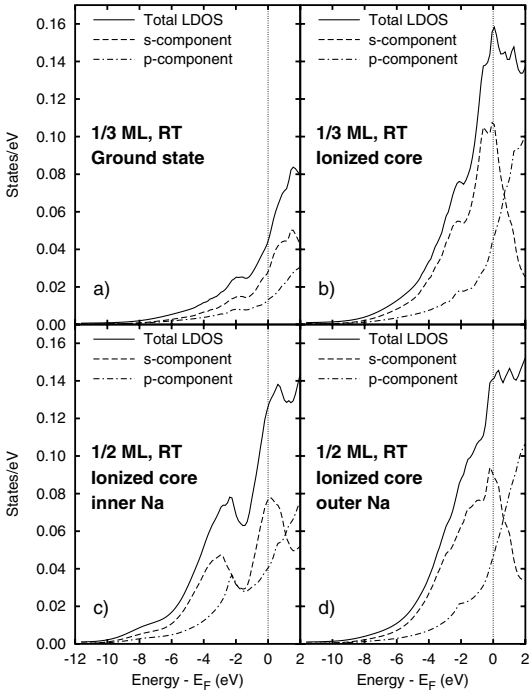

FIG. 3. Top panels: the Na $(\sqrt{3} \times \sqrt{3})R30\,^\circ$ phase ($1/3$ ML at RT); ground state LDOS [panel (a)] and core ionized LDOS [panel (b)] calculated around Na. Bottom panels: the Na (2×2) phase ($1/2$ ML at RT); core ionized LDOS's calculated around the inner Na atom [panel (c)] and the outer one [panel (d)].

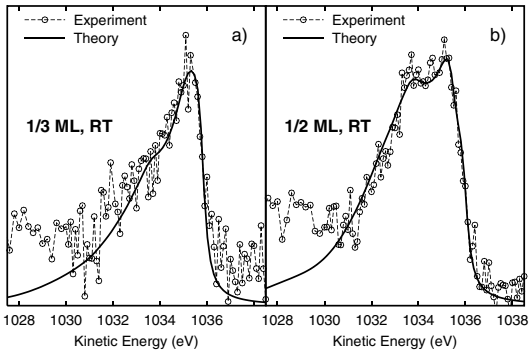

FIG. 4. Panel (a) the Na $(\sqrt{3} \times \sqrt{3})R30°$ phase (1/3 ML at RT). Calculated (solid line) and measured (circles) $KL_{2,3}V$ Auger profiles. The calculated curve, normalized to the experimental data, obtained convolving the Auger rate with a Lorentzian with half width $\Gamma = 0.42$ eV for the core hole lifetime and a Gaussian for nominal instrumental broadening. The measured one obtained after background subtraction. Panel (b) the Na (2×2) phase (1/2 ML at RT). Calculated (solid line) and measured (circles) $KL_{2,3}V$ Auger profiles. The calculated curve as in panel (a) but summing the contributions from the two inequivalent Na atoms (see text).

allow one to identify inequivalent chemisorption geometries.

Finally we compare the experimental and theoretical $KL_{2,3}V$ spectra in Fig. 4. From energy conservation, the calculated energy of the Auger electron emitted from the Fermi level is about 1035.3 eV and is fairly insensitive to the two Na adsorption phases. Its value is very close to the experimental one. The agreement between the two sets of results in Fig. 4 is impressive. For the 1/3 ML, in panel (a), both theoretical and experimental spectra display a main feature of the same shape and intensity. On the other hand, to fit the experiments for the 1/2 ML phase, it is necessary to sum up the contributions of the two theoretical spectra obtained from the inner and outer Na atoms, and eventually to take into account a shift between the calculated corresponding signals. The best fit was obtained by shifting the Auger spectrum of the outer atom by -0.5 eV, and assigning a weight of 3/8 to the outer Na atom signal and 5/8 to the inner one. The weight ratio between the two Na components is in agreement with the analysis of the relative height of the XPS signal (see Fig. 1). It is interesting to note that this result suggests a different population for the Na atoms in the two inequivalent sites.

In this Letter we have demonstrated the capability of CCV Auger line shapes to account for the geometry of different adsorption phases for a given atom on the same solid surface. This approach could be extended to core-valence-valence decays, too. In fact, DFT calculations can be employed to determine, via the LDOS, the Auger rates of a large class of adsorbate systems, provided that the width of the valence band of the solid is much larger than the on-site Coulomb interaction representing the final state correlation interaction between two valence holes. We also wish to stress that our theoretical method is not only able to determine qualitatively the line shapes of Auger spectra but is also potentially capable to predict features from different adsorbate components coexisting in the signal. While the former result has been verified experimentally, the latter one requires the use of coincidence techniques, a field of growing interest and expansion at synchrotron facilities [19]. In fact, photoelectron-Auger coincidence spectroscopy allows one to unequivocally associate every Auger feature with the originating core level photohole. In all these respects, this Letter should provide new perspectives for Auger spectroscopy.

We acknowledge R. Gotter for useful discussions and suggestions. This work was supported by the Italian MIUR through Grant No. 2003028141.

[1] M. Drescher, M. Hentschel, R. Kienberger, M. Uiberacker *et al.*, Nature (London) **419**, 803 (2002).
[2] V. I. Klimov, A. A. Mikhailovsky, D.W. McBranch, C. A. Leatherdale *et al.*, Science **287**, 1011 (2000).
[3] W. Olovsson, I. A. Abrikosov, B. Johansson, A. Newton *et al.*, Phys. Rev. Lett. **92**, 226406 (2004).
[4] J. N. Andersen, E. Lundgren, R. Nyholm, and M. Qvarford, Surf. Sci. **289**, 307 (1993).
[5] A. Schmalz, S. Aminpirooz, L. Becker, J. Haase *et al.*, Phys. Rev. Lett. **67**, 2163 (1991).
[6] J. Burchhardt, M. M. Nielsen, D. L. Adams, E. Lundgren *et al.*, Phys. Rev. Lett. **74**, 1617 (1995).
[7] C. Stampfl and M. Scheffler, Surf. Sci. **319**, L23 (1994).
[8] U. von Barth and G. Grossmann, Phys. Scr. **28**, 107 (1983).
[9] N. Bonini, M. I. Trioni, and G. P. Brivio, Phys. Rev. B **64**, 035424 (2001).
[10] A. J. Du, M. I. Trioni, G. P. Brivio, and N. Bonini, Surf. Sci. **545**, L753 (2003).
[11] P. Weightman, M. Davies, and J. E. Inglesfield, Phys. Rev. B **34**, 6843 (1986).
[12] J. E. Inglesfield, J. Phys. C **14**, 3795 (1981).
[13] H. Ishida, Phys. Rev. B **63**, 165409 (2001).
[14] L. Floreano, G. Naletto, D. Cvetko, R. Gotter *et al.*, Rev. Sci. Instrum. **70**, 3855 (1999).
[15] M. Kerkar, D. Fisher, D. P. Woodruff, R. G. Jones *et al.*, Surf. Sci. **278**, 246 (1992).
[16] H. Brune, J. Wintterlin, R. J. Behm, and G. Ertl, Phys. Rev. B **51**, 13592 (1995).
[17] S. Lizzit, A. Baraldi, A. Groso, K. Reuter *et al.*, Phys. Rev. B **63**, 205419 (2001).
[18] U. von Barth and G. Grossmann, Solid State Commun. **32**, 645 (1979).
[19] J. Danger, H. Magnan, D. Chandesris, P. Le Fèvre *et al.*, Phys. Rev. B **64**, 045110 (2001).